

Double vector meson production in photon - hadron interactions at hadronic colliders

V.P. Gonçalves^{1,2}, B.D. Moreira³ and F.S. Navarra³

¹ *Department of Astronomy and Theoretical Physics,
 Lund University, SE-223 62 Lund, Sweden*

² *High and Medium Energy Group,
 Instituto de Física e Matemática,
 Universidade Federal de Pelotas*

Caixa Postal 354, 96010-900, Pelotas, RS, Brazil.

³ *Instituto de Física, Universidade de São Paulo,
 C.P. 66318, 05315-970 São Paulo, SP, Brazil*

In this paper we analyse the double vector meson production in photon – hadron (γh) interactions at $pp/pA/AA$ collisions and present predictions for the $\rho\rho$, $J/\Psi J/\Psi$ and $\rho J/\Psi$ production considering the double scattering mechanism. We estimate the total cross sections and rapidity distributions at LHC energies and compare our results with the predictions for the double vector meson production in $\gamma\gamma$ interactions at hadronic colliders. We present predictions for the different rapidity ranges probed by the ALICE, ATLAS, CMS and LHCb Collaborations. Our results demonstrate that the $\rho\rho$ and $J/\Psi J/\Psi$ production in $PbPb$ collisions is dominated by the double scattering mechanism, while the two - photon mechanism dominates in pp collisions. Moreover, our results indicate that the analysis of the $\rho J/\Psi$ production at LHC can be useful to constrain the double scattering mechanism.

PACS numbers: 12.38.-t, 24.85.+p, 25.30.-c

Keywords: Quantum Chromodynamics, Double Vector Meson Production, Saturation effects.

Recent theoretical and experimental studies has demonstrated that hadronic colliders can also be considered photon – hadron and photon – photon colliders [1] which allow us to study the photon – induced interactions in a new kinematical range and probe e.g. the nuclear gluon distribution [2–6], the dynamics of the strong interactions [7–14], the Odderon [19, 20], the mechanism of quarkonium production [13–18] and the photon flux of the proton [21, 22]. In particular, the installation of forward detectors in the LHC [23, 24] should allows to separate more easily the exclusive processes, where the incident hadrons remain intact, allowing a detailed study of more complex final states as e.g. the exclusive production of two vector mesons explore other final states. Recent results from the LHCb Collaboration for the exclusive double J/Ψ production [25] has demonstrate that the experimental analysis of this process is feasible, motivating the improvement of the theoretical description of this process [26–29, 31]. In particular, in Ref. [31] we have revisited the double vector production in $\gamma\gamma$ interactions, proposed originally in Refs. [32–34], taking into account recent improvements in the description of the $\gamma\gamma \rightarrow VV$ ($V = \rho, J/\Psi$) cross section at low [28, 29] and high [30] energies. A typical diagram for this process is represented in Fig. 1. The results presented in Ref. [31] has demonstrated that the analysis of this process is feasible in hadronic collisions, mainly in pp collisions, and that its study may be useful to constrain the QCD dynamics at high energies, as proposed originally in Ref. [32]. However, double vector mesons can also be produced in photon – hadron (γh) interactions if a double scattering occurs in a same event, as represented in Fig. 2. The treatment of this double scattering mechanism (DSM) for γh interactions in heavy ion collisions was proposed originally in Ref. [35] and the double ρ production was recently discussed in detail in Ref. [36]. Such results demonstrated that the contribution of the double scattering mechanism is important for high energies, which motivates a more detailed analysis of this process. In this paper we extend these previous studies for the double J/Ψ and $\rho J/\Psi$ production in AA collisions and present, by the first time, predictions for the double vector meson in pp and pA collisions. Additionally, we compare our results for double vector meson production in γh interactions with those obtained in Ref. [31] for $\gamma\gamma$ interactions. As we will demonstrate below, the $\rho\rho$ and $J/\Psi J/\Psi$ production in $PbPb$ collisions is dominated by the double scattering mechanism, while the two - photon mechanism dominates in pp collisions. Moreover, our results indicate that the analysis of the $\rho J/\Psi$ production at LHC can be useful to constrain the double scattering mechanism.

Lets start our analysis presenting a brief review of the main concepts and formulas to describe the single and double

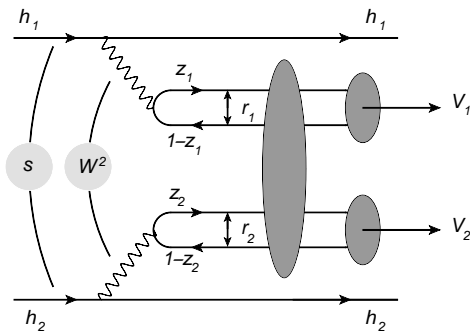


FIG. 1: Double vector meson production in $\gamma\gamma$ interactions at hadronic colliders in the color dipole picture.

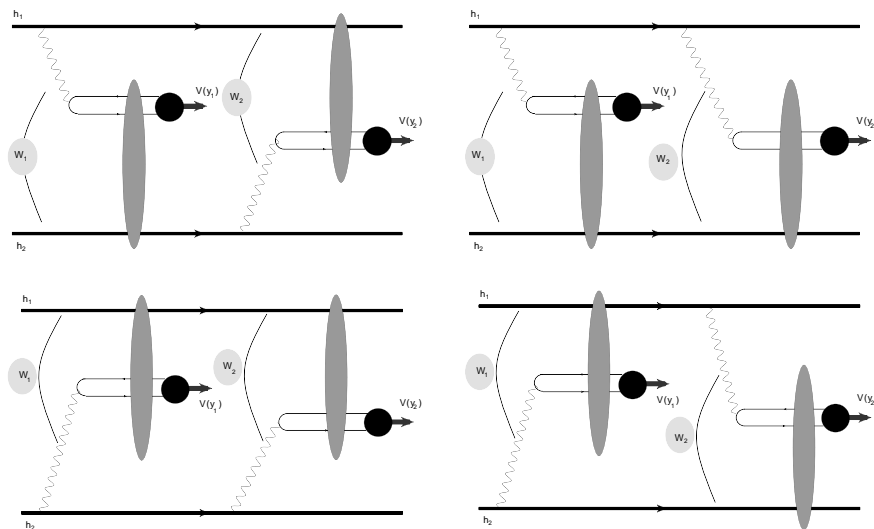


FIG. 2: Double vector meson production in γh interactions at hadronic colliders in the color dipole picture.

vector meson production in γh interactions at hadronic colliders. The basic idea in the photon-induced processes is that a ultra relativistic charged hadron (proton or nucleus) give rise to strong electromagnetic fields, such that the photon stemming from the electromagnetic field of one of the two colliding hadrons can interact with one photon of the other hadron (photon - photon process) or can interact directly with the other hadron (photon - hadron process) [1, 37]. In these processes the total cross section can be factorized in terms of the equivalent flux of photons into the hadron projectile and the photon-photon or photon-target production cross section. In this paper our main focus will be diffractive vector meson production in photon - hadron interactions in hadronic collisions. The differential cross sections for the production of a single vector meson V at rapidity y at fixed impact parameter b of the hadronic collision can be expressed as follows:

$$\frac{d\sigma [h_1 + h_2 \rightarrow h_1 \otimes V \otimes h_2]}{d^2b dy} = [\omega N_{h_1}(\omega, b) \sigma_{\gamma h_2 \rightarrow V \otimes h_2}(\omega)]_{\omega_L} + [\omega N_{h_2}(\omega, b) \sigma_{\gamma h_1 \rightarrow V \otimes h_1}(\omega)]_{\omega_R} \quad (1)$$

where the rapidity (y) of the vector meson in the final state is determined by the photon energy ω in the collider frame and by mass M_V of the vector meson [$y \propto \ln(\omega/M_V)$]. Moreover, $\sigma_{\gamma h_i \rightarrow V \otimes h_i}$ is the total cross section for the diffractive vector meson photoproduction, with the symbol \otimes representing the presence of a rapidity gap in the final state and $\omega_L (\propto e^{-y})$ and $\omega_R (\propto e^y)$ denoting photons from the h_1 and h_2 hadrons, respectively. One have that Eq. (1) takes into account that both incident hadrons can be source of photon which will interact with the other hadron. The equivalent photon spectrum $N(\omega, b)$ of a relativistic hadron for photons of energy ω at the distance \mathbf{b} to the hadron trajectory, defined in the plane transverse to the trajectory, can be expressed in terms of the charge form

factor F as follows

$$N(\omega, b) = \frac{Z^2 \alpha_{em}}{\pi^2} \frac{1}{b^2 \omega} \cdot \left[\int u^2 J_1(u) F \left(\sqrt{\frac{\left(\frac{b\omega}{\gamma_L}\right)^2 + u^2}{b^2}} \right) \frac{1}{\left(\frac{b\omega}{\gamma_L}\right)^2 + u^2} du \right]^2, \quad (2)$$

where γ_L is the Lorentz factor. The double vector meson production can occur if two γh interactions are present in the same event, as represented in Fig. 2. In order to treat this double - scattering mechanism we will follow the approach from Refs. [35, 36] that proposed that the double differential cross section for the production of a vector meson V_1 at rapidity y_1 and a second vector meson V_2 at rapidity y_2 will be given by

$$\frac{d^2 \sigma_{h_1 h_2 \rightarrow h_1 V_1 V_2 h_2}}{dy_1 dy_2} = \mathcal{C} \int_{b_{min}} \frac{d\sigma [h_1 + h_2 \rightarrow h_1 V_1 h_2]}{d^2 b dy_1} \times \frac{d\sigma [h_1 + h_2 \rightarrow h_1 V_2 h_2]}{d^2 b dy_2} d^2 b, \quad (3)$$

where \mathcal{C} is equal to 1 (1/2) for $V_1 \neq V_2$ ($V_1 = V_2$) and $b_{min} = R_{h_1} + R_{h_2}$ excludes the overlap between the colliding hadrons and allows to take into account only ultra peripheral collisions. Consequently, the double vector meson production can be easily estimated in terms of the cross sections for the single vector meson production, which is determined by the photon flux and the $\gamma h \rightarrow V h$ cross section.

In what follows we will consider the color dipole formalism to describe the diffractive vector meson photoproduction, which successfully describe the HERA data and recent LHC data [13, 14, 38]. In this approach the description of the single vector meson production can be factorized as follows: i) a photon is emitted by one of the incident hadrons, ii) the photon fluctuates into a quark-antiquark pair (the dipole), iii) this color dipole interact with the other hadron by the exchange of a color single state, denoted Pomeron (\mathbb{P}) and, iv) the pair converts into the vector meson final state. The $\gamma h \rightarrow V h$ cross section is given by

$$\sigma(\gamma h \rightarrow V h) = \int_{-\infty}^0 \frac{d\sigma}{dt} dt = \frac{1}{16\pi} \int_{-\infty}^0 |\mathcal{A}_T^{\gamma h \rightarrow V h}(x, \Delta)|^2 dt, \quad (4)$$

with the scattering amplitude is given by

$$\mathcal{A}_T^{\gamma h \rightarrow V h}(x, \Delta) = i \int dz d^2 \mathbf{r} d^2 \mathbf{b}_h e^{-i[\mathbf{b}_h - (1-z)\mathbf{r}] \cdot \Delta} (\Psi^{V*} \Psi)_T 2\mathcal{N}_h(x, \mathbf{r}, \mathbf{b}_h), \quad (5)$$

where $(\Psi^{V*} \Psi)_T$ denotes the overlap of the transverse photon and vector meson wave functions. The variable z ($1-z$) is the longitudinal momentum fractions of the quark (antiquark) and Δ denotes the transverse momentum lost by the outgoing pion ($t = -\Delta^2$). The variable \mathbf{b}_h is the transverse distance from the center of the target h to the center of mass of the $q\bar{q}$ dipole and the factor in the exponential arises when one takes into account non-forward corrections to the wave functions [39]. As in our previous studies [13, 14] in what follows we will assume that the vector meson is predominantly a quark-antiquark state and that the spin and polarization structure is the same as in the photon [40–43] (for other approaches see, for example, Ref. [44]). As a consequence, the overlap between the photon and the vector meson wave function, for the transversely polarized case, is given by (For details see Ref. [45])

$$(\Psi_V^* \Psi)_T = \frac{\hat{e}_f e}{4\pi} \frac{N_c}{\pi z(1-z)} \{m_f^2 K_0(\epsilon r) \phi_T(r, z) - [z^2 + (1-z)^2] \epsilon K_1(\epsilon r) \partial_r \phi_T(r, z)\}, \quad (6)$$

where \hat{e}_f is the effective charge of the vector meson, m_f is the quark mass, $N_c = 3$, $\epsilon^2 = z(1-z)Q^2 + m_f^2$ and $\phi_i(r, z)$ define the scalar parts of the vector meson wave functions. In the Gauss-LC model one have that

$$\phi_T(r, z) = N_T [z(1-z)]^2 \exp(-r^2/2R_T^2). \quad (7)$$

with the parameters N_T and R_T being determined by the normalization condition of the wave function and by the meson decay width (For details see Table 1 in Ref. [14]). It is important to emphasize that predictions based on this model for the wave functions have been tested with success in ep and ultra peripheral hadronic collisions (See, e. g. Refs. [13, 14, 38, 46]). Moreover, $\mathcal{N}_h(x, \mathbf{r}, \mathbf{b}_h)$ denotes the non-forward scattering amplitude of a dipole of size \mathbf{r} on the hadron h , which is directly related to the QCD dynamics. In what follows we will assume that for the proton case $\mathcal{N}_p(x, \mathbf{r}, \mathbf{b}_p)$ is given by the bCGC model proposed in Ref. [45], which improves the Iancu - Itakura - Munier (IIM) model [47] with the inclusion of the impact parameter dependence in the dipole - proton scattering amplitude. Following [45] we have:

$$\mathcal{N}_p(x, \mathbf{r}, \mathbf{b}_p) = \begin{cases} \mathcal{N}_0 \left(\frac{r Q_{s,p}}{2} \right)^{2\left(\gamma_s + \frac{\ln(2/r Q_{s,p})}{\kappa \lambda Y}\right)} & r Q_{s,p} \leq 2 \\ 1 - \exp[-A \ln^2(B r Q_{s,p})] & r Q_{s,p} > 2 \end{cases} \quad (8)$$

with $Y = \ln(1/x)$ and $\kappa = \chi''(\gamma_s)/\chi'(\gamma_s)$, where χ is the LO BFKL characteristic function [48]. The coefficients A and B are determined uniquely from the condition that $\mathcal{N}_p(x, \mathbf{r}, \mathbf{b}_p)$, and its derivative with respect to rQ_s , are continuous at $rQ_s = 2$. In this model, the proton saturation scale $Q_{s,p}$ depends on the impact parameter:

$$Q_{s,p} \equiv Q_{s,p}(x, \mathbf{b}_p) = \left(\frac{x_0}{x}\right)^{\frac{\lambda}{2}} \left[\exp\left(-\frac{b_p^2}{2B_{CGC}}\right) \right]^{\frac{1}{2\gamma_s}}. \quad (9)$$

The parameter B_{CGC} was adjusted to give a good description of the t -dependence of exclusive J/ψ photoproduction. The factors \mathcal{N}_0 , x_0 , λ and γ_s were taken to be free. Recently the parameters of this model have been updated in Ref. [38] (considering the recently released high precision combined HERA data), giving $\gamma_s = 0.6599$, $B_{CGC} = 5.5 \text{ GeV}^{-2}$, $\mathcal{N}_0 = 0.3358$, $x_0 = 0.00105 \times 10^{-5}$ and $\lambda = 0.2063$. As demonstrate in Ref. [49], this phenomenological dipole describes quite well the HERA data for the exclusive ρ and J/Ψ production. Moreover, the results from Refs. [13, 14] demonstrated that this model allows to describe the recent LHC data for the exclusive vector meson photoproduction in pp and pPb collisions. Another motivation to use the bCGC model, is that this model is based on the CGC physics, which was used in Ref. [31] to estimate the double vector meson production in $\gamma\gamma$ interactions. A common approach for the QCD dynamics in $\gamma\gamma$ and γh interactions is important to minimize the theoretical uncertainty and to perform a realistic comparison between the predictions of the two different mechanisms for the double vector production. In order to describe the vector meson production in γA interactions we need to specify the forward dipole - nucleus scattering amplitude, $\mathcal{N}_A(x, \mathbf{r}, \mathbf{b}_A)$. Following [13] we will use in our calculations the model proposed in Ref. [50], which describes the current experimental data on the nuclear structure function as well as includes the impact parameter dependence in the dipole nucleus cross section. In this model the forward dipole-nucleus amplitude is given by

$$\mathcal{N}_A(x, \mathbf{r}, \mathbf{b}_A) = 1 - \exp\left[-\frac{1}{2} \sigma_{dp}(x, \mathbf{r}^2) T_A(\mathbf{b}_A)\right], \quad (10)$$

where σ_{dp} is the dipole-proton cross section given by

$$\sigma_{dp}(x, \mathbf{r}^2) = 2 \int d^2\mathbf{b}_p \mathcal{N}_p(x, \mathbf{r}, \mathbf{b}_p) \quad (11)$$

and $T_A(\mathbf{b}_A)$ is the nuclear profile function, which is obtained from a 3-parameter Fermi distribution for the nuclear density normalized to A . The above equation sums up all the multiple elastic rescattering diagrams of the $q\bar{q}$ pair and is justified for large coherence length, where the transverse separation \mathbf{r} of partons in the multiparton Fock state of the photon becomes a conserved quantity, *i.e.* the size of the pair \mathbf{r} becomes eigenvalue of the scattering matrix.

In the case of the double vector meson production in $\gamma\gamma$ interactions at hadronic colliders, represented in Fig. 1, we have that the total cross section is given by (For details see Ref. [31])

$$\sigma(h_1 h_2 \rightarrow h_1 \otimes V_1 V_2 \otimes h_2; s) = \int \hat{\sigma}(\gamma\gamma \rightarrow V_1 V_2; W_{\gamma\gamma}) N(\omega_1, \mathbf{b}_1) N(\omega_2, \mathbf{b}_2) S_{abs}^2(\mathbf{b}) \frac{W_{\gamma\gamma}}{2} d^2\mathbf{b}_1 d^2\mathbf{b}_2 dW_{\gamma\gamma} dY \quad (12)$$

where ω_1 and ω_2 are the photon energies, $W_{\gamma\gamma} = \sqrt{4\omega_1\omega_2}$ is the invariant mass of the $\gamma\gamma$ system and Y is the rapidity of the outgoing double meson system. Moreover, $S_{abs}^2(\mathbf{b})$ is the absorption factor, given in what follows by

$$S_{abs}^2(\mathbf{b}) = \Theta(|\mathbf{b}| - R_{h_1} - R_{h_2}) = \Theta(|\mathbf{b}_1 - \mathbf{b}_2| - R_{h_1} - R_{h_2}), \quad (13)$$

where R_{h_i} is the radius of the hadron h_i ($i = 1, 2$). In the dipole picture, the $\gamma\gamma \rightarrow V_1 V_2$ cross section can be expressed as follows

$$\sigma(\gamma\gamma \rightarrow V_1 V_2) = \frac{[\text{Im} \mathcal{A}(W_{\gamma\gamma}^2, t=0)]^2}{16\pi B_{V_1 V_2}}, \quad (14)$$

where we have approximated the t -dependence of the differential cross section by an exponential with $B_{V_1 V_2}$ being the slope parameter. The imaginary part of the amplitude at zero momentum transfer $\mathcal{A}(W_{\gamma\gamma}^2, t=0)$ reads as

$$\begin{aligned} \text{Im} \mathcal{A}(\gamma\gamma \rightarrow V_1 V_2) &= \int dz_1 d^2\mathbf{r}_1 [\Psi^\gamma(z_1, \mathbf{r}_1) \Psi^{V_1^*}(z_1, \mathbf{r}_1)]_T \\ &\times \int dz_2 d^2\mathbf{r}_2 [\Psi^\gamma(z_2, \mathbf{r}_2) \Psi^{V_2^*}(z_2, \mathbf{r}_2)]_T \sigma_{dd}(\mathbf{r}_1, \mathbf{r}_2, Y), \end{aligned} \quad (15)$$

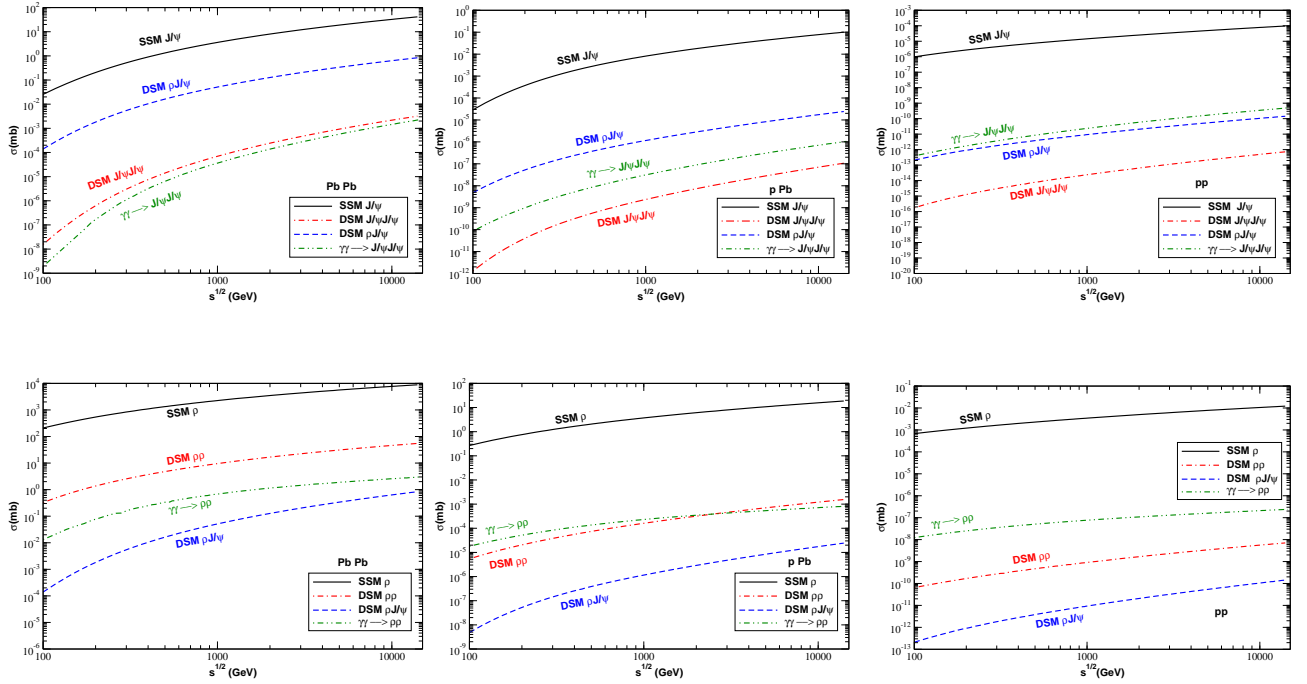


FIG. 3: Energy dependence for the $J/\Psi J/\Psi$ (upper panels) and $\rho\rho$ (lower panels) production in γh and $\gamma\gamma$ interactions in $PbPb$ (left panels), pPb (middle panels) and pp (right panels) collisions. The predictions associated to the double scattering mechanism are denoted DSM. For comparison the predictions for the single vector meson production, denoted SSM, are also shown.

Final state	Mechanism	$PbPb$	$PbPb$	pPb	pp	pp
		$\sqrt{s} = 2.76$ TeV	$\sqrt{s} = 5.5$ TeV	$\sqrt{s} = 5$ TeV	$\sqrt{s} = 7$ TeV	$\sqrt{s} = 14$ TeV
$J/\Psi J/\Psi$	DSM	402.301 nb	1054.951 nb	28.473 pb	3.223×10^{-4} pb	7.256×10^{-4} pb
	$\gamma\gamma$	235.565 nb	658.589 nb	310.194 pb	0.2412 pb	0.4793 pb
$\rho\rho$	DSM	21.150 mb	29.421 mb	702.595 nb	4.354 pb	7.083 pb
	$\gamma\gamma$	1.389 mb	1.973 mb	536.432 nb	182.442 pb	237.006 pb
$\rho J/\Psi$	DSM	0.18 mb	0.35 mb	8.929 nb	7.469×10^{-2} pb	14.288×10^{-2} pb

TABLE I: Total cross sections for the double vector meson production considering the double scattering and two - photon mechanisms and different center - of - mass energies considering the full kinematical range covered by the LHC.

where Ψ^γ and Ψ^{V_i} are the light-cone wave functions of the photon and vector meson, respectively, and T the transverse polarization. The variable \mathbf{r}_1 defines the relative transverse separation of the pair (dipole) and z_1 ($1 - z_1$) is the longitudinal momentum fraction of the quark (antiquark). Similar definitions are valid for \mathbf{r}_2 and z_2 . Moreover, σ_{dd} is the dipole - dipole cross section, which can be estimated taking into account the nonlinear effects in the QCD dynamics. In what follows, we assume the Gauss-LC model for the vector meson wave functions and estimate σ_{dd} using the approach proposed in Refs. [31, 51], which is based on the CGC physics. We refer the reader to the Ref. [31] for more details about the double vector meson production in $\gamma\gamma$ interactions.

In what follows we present our predictions for the rapidity distributions and total cross sections for the $\rho\rho$, $\rho J/\Psi$ and $J/\Psi J/\Psi$ production in γh interactions at $pp/pPb/PbPb$ collisions. We will denote the predictions associated to the double scattering mechanics by DSM hereafter. Following Ref. [36] we will estimate the equivalent photon spectra for $A = Pb$ assuming the nucleus as a point - like object, i.e. $F(q^2) = 1$. In the proton case, we will take $F(q^2) = 1/[1 + q^2/(0.71\text{GeV}^2)]^2$ and $R_p = 0.7$ fm as in Ref. [31]. Moreover, we will compare our predictions for the $J/\Psi J/\Psi$ and $\rho\rho$ production with the results obtained in Ref. [31] for the production of these final states in $\gamma\gamma$ interactions. In Fig. 3 we present our predictions for the energy dependence of the total cross sections for the double vector meson production in γh and $\gamma\gamma$ interactions. For the double J/Ψ production (upper panels), the double scattering mechanism becomes competitive with the two - photon one only in $PbPb$ collisions, being a factor 10 (100) smaller in pPb (pp) collisions. In particular, for pp collisions, the DSM contribution is negligible. On the other hand, our results demonstrate that the associated production of a J/Ψ and a ρ meson by the double scattering mechanism is

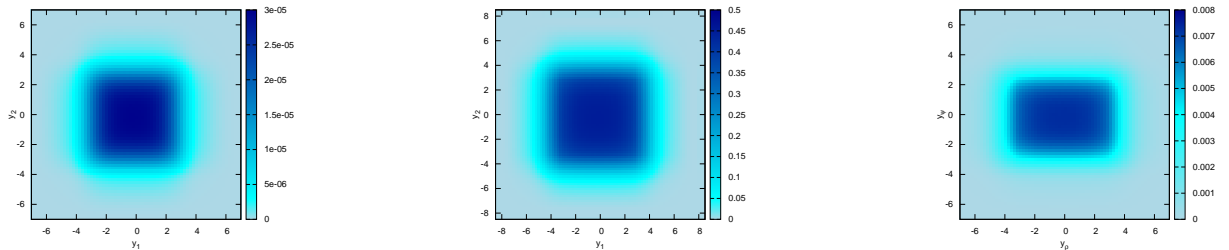


FIG. 4: Double differential rapidity distribution for the $J/\Psi J/\Psi$ (left panel), $\rho\rho$ (middle panel) and $\rho J/\Psi$ (right panel) production in γh interactions at $PbPb$ collisions ($\sqrt{s} = 5.5$ TeV) by the double scattering mechanism.

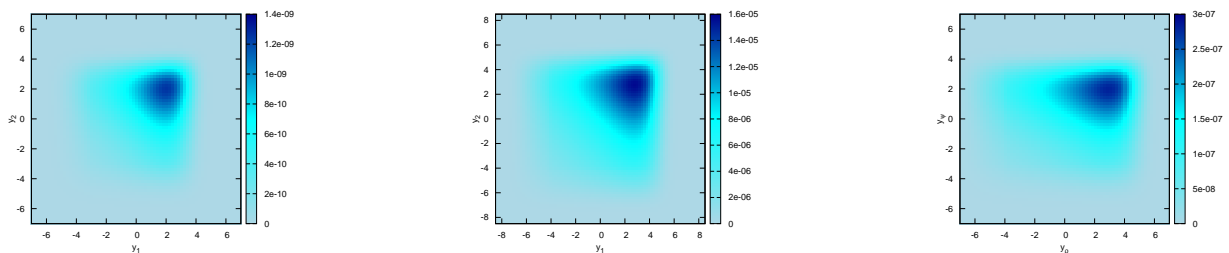


FIG. 5: Double differential rapidity distribution for the $J/\Psi J/\Psi$ (left panel), $\rho\rho$ (middle panel) and $\rho J/\Psi$ (right panel) production in γh interactions at pPb collisions ($\sqrt{s} = 5$ TeV) by the double scattering mechanism.

important the LHC range. It is important to emphasize that this final state also can be produced by $\gamma\gamma$ interactions. However, as its contribution in hadronic collisions still is an open question due to the current large uncertainty on the normalization of the $\gamma\gamma \rightarrow \rho J/\Psi$ cross section (For a detailed discussion see Ref. [30]), we do not present the associated predictions. In the case of the double ρ production (lower panels), the double scattering mechanism is dominant in $PbPb$ collisions, in agreement with the results presented in Ref. [36]. On the other hand, the contribution of the double scattering and two-photon mechanisms are similar in pPb collisions, while the $\gamma\gamma$ dominates in the pp collisions. These results demonstrate that the analysis of this final state in $PbPb/pPb/pp$ can be useful to disentangle the different mechanisms for the $\rho\rho$ production. The corresponding total cross sections at different values of the center-of-mass energy are presented in Table I considering the full kinematical range covered by the LHC.

In Figs. 4 and 5 we present our predictions for the rapidity distributions for the double vector meson production by the double scattering mechanism in $PbPb$ and pPb collisions, respectively. For $PbPb$ collisions, as expected, one has symmetric distributions for the $J/\Psi J/\Psi$ and $\rho\rho$ production. On the other hand, in the case of the $\rho J/\Psi$ production, the distribution is asymmetric, being wider for the rapidity associated to the ρ meson. In the case of pPb collisions, one has that the photon flux of the nucleus is amplified by a factor Z^2 in comparison to the photon flux associated to the proton. As a consequence, the double scattering mechanism is dominated by γh interactions where the photons are emitted by the nucleus. The contribution associated to one photon emitted by the nucleus and the other by the proton is suppressed by a factor Z^2 , while the contribution associated to γh interactions with photons emitted by the proton is suppressed by a factor Z^4 . It implies that the rapidity distributions are asymmetric for all final states considered (See Fig. 5). Similarly as observed in $PbPb$ collisions, the rapidity distribution associated to the ρ meson is wider in comparison to the J/Ψ one.

Finally, in Table II we present our predictions for the total cross sections for the double vector production by the double scattering mechanism in $PbPb$ and pPb collisions considering the rapidity ranges covered by the ATLAS, CMS, ALICE and LHCb Collaborations. In the particular case of the ALICE Collaboration we estimate the cross sections considering: (a) that both mesons are produced in the range $-1 < y_{1,2} < 1$ (denoted ALICE1 in the Table) and (b) that one meson is produced in the range $-1 < y_1 < 1$ and the other in the range $-3.6 < y_2 < -2.6$ (denoted ALICE2). For the $\rho J/\Psi$ production in the ALICE2 range, we present our results for the two possible configurations: $(y_1, y_2) = (y_\rho, y_{J/\Psi})$ and $(y_1, y_2) = (y_{J/\Psi}, y_\rho)$, with the results associated to the latter one being presented in parenthesis in Table II. We predict large values for the total cross sections, in particular, for the $\rho\rho$ and

Final state		LHCb	ATLAS/CMS	ALICE1	ALICE2
		$2 < y_{1,2} < 4.5$	$-2 < y_{1,2} < 2$	$-1 < y_{1,2} < 1$	$-1 < y_1 < 1$ and $-3.6 < y_2 < -2.6$
$J/\Psi J/\Psi$	$PbPb$ ($\sqrt{s} = 2.76$ TeV)	5.51 nb	234.94 nb	69.91 nb	6.94 nb
	$PbPb$ ($\sqrt{s} = 5.5$ TeV)	30.85 nb	446.11 nb	118.03 nb	25.45 nb
	pPb ($\sqrt{s} = 5$ TeV)	3.25 pb	8.87 pb	2.16 pb	0.37 pb
$\rho\rho$	$PbPb$ ($\sqrt{s} = 2.76$ TeV)	0.93 mb	6.08 mb	1.58 mb	0.54 mb
	$PbPb$ ($\sqrt{s} = 5.5$ TeV)	1.50 mb	7.06 mb	1.79 mb	0.73 mb
	pPb ($\sqrt{s} = 5$ TeV)	84.09 nb	122.03 nb	30.11 nb	8.53 nb
$\rho J/\Psi$	$PbPb$ ($\sqrt{s} = 2.76$ TeV)	4.48 μ b	75.17 μ b	20.94 μ b	2.06 (7.25) μ b
	$PbPb$ ($\sqrt{s} = 5.5$ TeV)	13.42 μ b	112.00 μ b	29.06 μ b	6.21 (11.86) μ b
	pPb ($\sqrt{s} = 5$ TeV)	1.02 nb	2.08 nb	0.51 nb	87.31 (144.56) pb

TABLE II: Total cross sections for the double vector meson production by the double scattering mechanism (DSM) for different center - of - mass energies considering the distinct phase space in rapidity covered by the ALICE, ATLAS, CMS and LHCb Collaborations.

$\rho J/\Psi$ production in $PbPb$ collisions, in the phase space covered by the different collaborations. Consequently, we believe that the analysis of these different final states is feasible in the future, which will allow to probe the double scattering mechanism at the LHC.

Let us summarize our main conclusions. In recent years, a series of studies have discussed in detail the treatment of the total cross section and the exclusive production of different final states in $\gamma\gamma$ and γh interactions considering very distinct theoretical approaches. In particular, recent results for the double vector meson production in $\gamma\gamma$ interactions at hadronic colliders has demonstrated that this process can be used to constrain the QCD dynamics at high energies. However, this final state can also be generated if double γh interactions are present in the same event. In this paper we have estimated the magnitude of this contribution for the $J/\Psi J/\Psi$, $\rho\rho$ and $\rho J/\Psi$ production in $PbPb/pPb/pp$ collisions. We have treated the double scattering and two - photon mechanisms using the dipole formalism and a same approach for the QCD dynamics and the vector meson wave function. Our results indicated that the DSM contribution is dominant for the $J/\Psi J/\Psi$ and $\rho\rho$ production in $PbPb$ collisions. On the other hand, the two - photon production dominates the double J/Ψ production in pPb and pp collisions. In the case of the double ρ production, the DSM and two - photon contributions are similar in pPb collisions, with the two - photon being dominant in pp collisions. Therefore, the analysis of double vector production considering different projectiles can be useful to disentangle the different mechanisms of production. In particular, the analysis of the DPS production in heavy ion collisions can be used to complement our understanding of the description of the diffractive vector meson photoproduction. Moreover, our results demonstrated that the DPS $\rho J/\Psi$ production is large in the LHC kinematical range. Finally, our predictions for the double vector meson production in the phase space covered by the different experimental collaborations at the LHC indicate that the study of the double vector meson production is feasible in the future.

Note added in the proof: One month after the submission of this paper, a report has appeared [52] where it has been estimated the exclusive double ρ production in pp collisions. The total cross section was estimated in [52] taking into account pomeron and reggeon exchanges and considering the tensor pomeron model proposed in Ref. [53] and discussed in detail in Ref. [54]. The cross sections found in [52] are more than three orders of magnitude larger than our predictions. Therefore, the double ρ production in pp collisions is predicted to be dominated by pomeron - pomeron interactions, which implies that the analysis of this process can be useful to probe the tensor pomeron model. An alternative to study the photon - induced $\rho\rho$ production in pp collisions analysed here is the reconstruction of the entire event with a cut on the summed transverse momentum of the event. As the typical photon virtualities are very small, the hadron scattering angles are very low. Consequently, we expect a different transverse momentum distribution of the scattered hadrons, with pomeron - pomeron interactions predicting larger p_T values. Surely this subject deserve a more detailed analysis in the future. Finally, it is important to emphasize that in contrast to pp collisions, the photon - induced interactions are expected to be dominant in $pA(AA)$ collisions due to the Z^2 (Z^4) enhancement associated to the presence of nuclear photon flux.

Acknowledgments

VPG thanks G. Contreras, S. Klein, R. McNulty and D. Tapia Takaki by useful discussions. This work was partially financed by the Brazilian funding agencies CNPq, CAPES, FAPERGS and FAPESP.

-
- [1] C. A. Bertulani and G. Baur, Phys. Rep. **163**, 299 (1988); G. Baur, K. Hencken, D. Trautmann, S. Sadovsky, Y. Kharlov, Phys. Rep. **364**, 359 (2002); V. P. Goncalves and M. V. T. Machado, Mod. Phys. Lett. A **19**, 2525 (2004); C. A. Bertulani, S. R. Klein and J. Nystrand, Ann. Rev. Nucl. Part. Sci. **55**, 271 (2005); K. Hencken *et al.*, Phys. Rept. **458**, 1 (2008).
- [2] V. P. Goncalves and C. A. Bertulani, Phys. Rev. C **65**, 054905 (2002).
- [3] A. L. Ayala Filho, V. P. Goncalves and M. T. Griep, Phys. Rev. C **78**, 044904 (2008)
- [4] A. Adeluyi and C. Bertulani, Phys. Rev. C **84**, 024916 (2011); Phys. Rev. C **85**, 044904 (2012)
- [5] V. Guzey and M. Zhalov, JHEP **1310**, 207 (2013); JHEP **1402**, 046 (2014).
- [6] V. P. Goncalves, L. A. S. Martins and W. K. Sauter, Eur. Phys. J. C **76**, no. 2, 97 (2016)
- [7] V. P. Goncalves and M. V. T. Machado, Eur. Phys. J. C **40**, 519 (2005).
- [8] V. P. Goncalves and M. V. T. Machado, Phys. Rev. C **73**, 044902 (2006); Phys. Rev. D **77**, 014037 (2008); Phys. Rev. C **80**, 054901 (2009).
- [9] V. P. Goncalves and M. V. T. Machado, Phys. Rev. C **84**, 011902 (2011)
- [10] L. Motyka and G. Watt, Phys. Rev. D **78**, 014023 (2008)
- [11] T. Lappi and H. Mantysaari, Phys. Rev. C **87**, 032201 (2013)
- [12] M. B. Gay Ducati, M. T. Griep and M. V. T. Machado, Phys. Rev. D **88**, 017504 (2013); Phys. Rev. C **88**, 014910 (2013).
- [13] V. P. Goncalves, B. D. Moreira and F. S. Navarra, Phys. Rev. C **90**, no. 1, 015203 (2014).
- [14] V. P. Goncalves, B. D. Moreira and F. S. Navarra, Phys. Lett. B **742**, 172 (2015).
- [15] W. Schafer and A. Szczurek, Phys. Rev. D **76**, 094014 (2007); A. Rybarska, W. Schafer and A. Szczurek, Phys. Lett. B **668**, 126 (2008); A. Cisek, W. Schafer and A. Szczurek, Phys. Rev. C **86**, 014905 (2012)
- [16] V. P. Goncalves and M. M. Machado, Eur. Phys. J. C **72**, 2231 (2012)
- [17] V. P. Goncalves and M. M. Machado, Eur. Phys. J. A **50**, 72 (2014)
- [18] A. Cisek, W. Schafer and A. Szczurek, JHEP **1504**, 159 (2015)
- [19] V. P. Goncalves, Nucl. Phys. A **902**, 32 (2013)
- [20] V. P. Goncalves and W. K. Sauter, Phys. Rev. D **91**, no. 9, 094014 (2015)
- [21] V. P. Goncalves and G. G. da Silveira, Phys. Rev. D **91**, no. 5, 054013 (2015)
- [22] G. G. da Silveira and V. P. Goncalves, Phys. Rev. D **92**, no. 1, 014013 (2015)
- [23] The CMS and TOTEM Collaborations, CMS-TOTEM Precision Proton Spectrometer Technical Design Report, <http://cds.cern.ch/record/1753795>.
- [24] M. Tasevsky [ATLAS Collaboration], AIP Conf. Proc. **1654**, 090001 (2015).
- [25] R. Aaij *et al.* [LHCb Collaboration], J. Phys. G **41**, 115002 (2014)
- [26] L. A. Harland-Lang, V. A. Khoze and M. G. Ryskin, J. Phys. G **42**, no. 5, 055001 (2015)
- [27] C. Brenner Mariotto and V. P. Goncalves, Phys. Rev. D **91**, no. 11, 114002 (2015)
- [28] M. Klusek, W. Schafer and A. Szczurek, Phys. Lett. B **674**, 92 (2009)
- [29] S. Baranov, A. Cisek, M. Klusek-Gawenda, W. Schafer and A. Szczurek, Eur. Phys. J. C **73**, no. 2, 2335 (2013)
- [30] F. Carvalho, V. P. Goncalves, B. D. Moreira and F. S. Navarra, Eur. Phys. J. C **75**, no. 8, 392 (2015)
- [31] V. P. Goncalves, B. D. Moreira and F. S. Navarra, Eur. Phys. J. C **76**, no. 3, 103 (2016)
- [32] V. P. Goncalves and M. V. T. Machado, Eur. Phys. J. C **28**, 71 (2003)
- [33] V. P. Goncalves and M. V. T. Machado, Eur. Phys. J. C **29**, 271 (2003)
- [34] V. P. Goncalves, M. V. T. Machado and W. K. Sauter, Eur. Phys. J. C **46**, 219 (2006)
- [35] S. R. Klein, J. Nystrand, Phys. Rev. C **60**, 014903 (1999).
- [36] M. Klusek-Gawenda and A. Szczurek, Phys. Rev. C **89**, 024912 (2014)
- [37] V. M. Budnev, I. F. Ginzburg, G. V. Meledin and V. G. Serbo, Phys. Rept. **15**, 181 (1975).
- [38] A. Rezaeian and I. Schmidt, Phys. Rev. D **88**, 074016 (2013)
- [39] J. Bartels, K. Golec-Biernat and K. Peters, Acta Phys. Polon. B **34**, 3051 (2003)
- [40] H. G. Dosch, T. Gousset, G. Kulzinger and H. J. Pirner, Phys. Rev. D **55**, 2602 (1997).
- [41] J. Nemchik, N. N. Nikolaev, E. Predazzi and B. G. Zakharov, Z. Phys. C **75**, 71 (1997)
- [42] J. R. Forshaw, R. Sandapen and G. Shaw, Phys. Rev. D **69**, 094013 (2004)
- [43] H. Kowalski and D. Teaney, Phys. Rev. D **68**, 114005 (2003)
- [44] J. P. B. C. de Melo and T. Frederico, Phys. Rev. C **55**, 2043 (1997).
- [45] H. Kowalski, L. Motyka and G. Watt, Phys. Rev. D **74**, 074016 (2006)
- [46] V. P. Goncalves, M. V. T. Machado and A. R. Meneses, Eur. Phys. J. C **68**, 133 (2010).
- [47] E. Iancu, K. Itakura, S. Munier, Phys. Lett. B **590**, 199 (2004).
- [48] L. N. Lipatov, Sov. J. Nucl. Phys. **23**, 338 (1976); E. A. Kuraev, L. N. Lipatov, V. S. Fadin, Sov. Phys. JETP **44**, 443 (1976); E. A. Kuraev, L. N. Lipatov, V. S. Fadin, Sov. Phys. JETP **45**, 199 (1977); I. I. Balitsky, L. N. Lipatov, Sov. J. Nucl. Phys. **28**, 822 (1978).
- [49] N. Armesto and A. H. Rezaeian, Phys. Rev. D **90**, no. 5, 054003 (2014)
- [50] N. Armesto, Eur. Phys. J. C **26**, 35 (2002).
- [51] V. P. Goncalves, M. S. Kugeratski, E. R. Cazaroto, F. Carvalho and F. S. Navarra, Eur. Phys. J. C **71**, 1779 (2011).

- [52] P. Lebiedowicz, O. Nachtmann and A. Szczurek, arXiv:1606.05126 [hep-ph].
- [53] C. Ewerz, M. Maniatis and O. Nachtmann, *Annals Phys.* **342**, 31 (2014)
- [54] P. Lebiedowicz, O. Nachtmann and A. Szczurek, *Annals Phys.* **344**, 301 (2014)